Considering Spherical Aberration using an Optical Ray Tracer designed with OOP

Isabelle Grenville
Blackett Laboratory, Department of Physics, Imperial College London

This report investigates how to construct an optical ray tracer using object-oriented programming (OOP). From this, the effects of refraction and diffraction are considered by modelling a single spherical surface, and a plano-convex lens in two different orientations. A bundle of rays with a beam diameter of 10 mm, and wavelength of 588 nm, is propagated through the three lens scenarios. The root-mean-square (RMS) of the spot radius at the focal point is calculated via a paraxial approximation to consider the extent of spherical aberration. Of all three lenses, the most effective at reducing spherical aberration is found to be the plano-convex singlet lens with the convex surface facing the input. Finally, the diffraction limit of the beam radius is found for each lens model.

I. Introduction

Ray tracing is used to define the path of waves through a system. The method has been integral to two main bodies of work: analysing optical systems and generating 3D images. Computer programs which simulate an optical ray tracer originated in the 1960s. [1]

In this report, the propagation of light rays through 3D models of optical elements is analysed and tested to investigate the imaging performance of simple lens systems.

II. Theory

A. Refracting surfaces

The shape of an optical surface tends to be spherical or planar in design. A spherical refracting surface, restricted to be centred on the optical axis (z axis), can be parametrised by the following:

Parameter	Description
$\mathbf{z_0}$	The intercept of the surface with the optical axis
curvature	The curvature of the surface
$\mathbf{n_1}, \mathbf{n_2}$	The refractive indices on each side of the medium
aperture radius	The maximum perpendicular displacement of the surface from the optical axis

Additionally, the curvature of the surface can be positive or negative, depending on whether the surface is convex or concave. The convention used in this report is that a negative curvature corresponds to a concave lens. Furthermore, a curvature of zero represents a plane surface. The magnitude of the curvature is equivalent to:

$$curvature = \frac{1}{radius\ of\ curvature}. \quad (1)$$

These parameters are represented graphically in Figure 1.

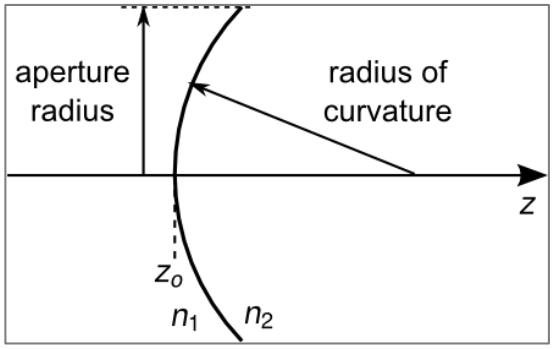

Figure 1 shows the parameters used to define an optical curve, centred along the optical axis (z axis). Graphic taken from [2].

B. Snell's Law

Light rays that encounter the surface of a lens undergo refraction, according to Snell's law:

$$n_1 sin\theta_1 = n_2 sin\theta_2 \quad (2)$$

where θ_1 and θ_2 are the angle of incidence and the angle of refraction, respectively, and n_1 is the refractive index of the medium before refraction and n_2 is the refractive index of the medium after refraction. This is illustrated in Figure 2.

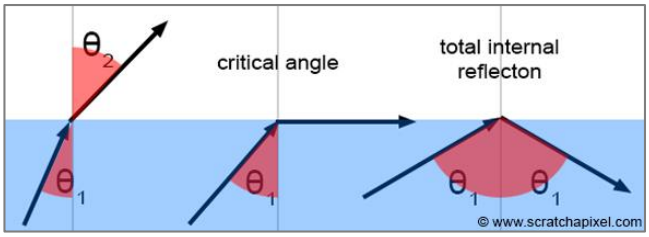

Figure 2 shows the effect of an incident ray refracting at the interface between two media, hitting the interface at the critical angle, and reflecting at the interface. Graphic taken from [3].

As shown in the diagram, beyond the critical angle, a light ray will be subject to total internal reflection. This occurs when

$$sin\theta_1 > \frac{n_2}{n_1}. \quad (3)$$

C. Lensmaker's Equation

The focal length of a lens can be calculated using the lensmaker's equation. For a thin lens in air, this can be approximated to be

$$\frac{1}{f} \approx (n-1)\left[\frac{1}{R_1} - \frac{1}{R_2}\right], \tag{4}$$

where f is the focal length of the lens, n is the refractive index of the material, R_1 is the radius of curvature of the lens surface closer to the light source, and R_2 is the radius of curvature of the lens surface farther from the light source. [4]

D. Spherical Aberration

An incident plane wave is represented by a collimated beam of rays, parallel to the optical axis. An ideal spherical surface would refract the rays such that they converge at a single point. This does not occur due to spherical aberration.

Spherical aberration can be defined as the effect of light rays not following the paraxial approximation. [5] A paraxial ray is one which is incident very close to the optical axis. This ray will cross the optical axis at the paraxial focus which represents the ideal focal point in the limit of a small beam radius.

However, a marginal ray – which is incident near the edge of the lens – will not cross the axis at this point. The further away the ray is from the optical axis, the less well it will refract according to the paraxial approximation. This is well represented by Figure 3 which shows the rays crossing the optical axis at varying points.

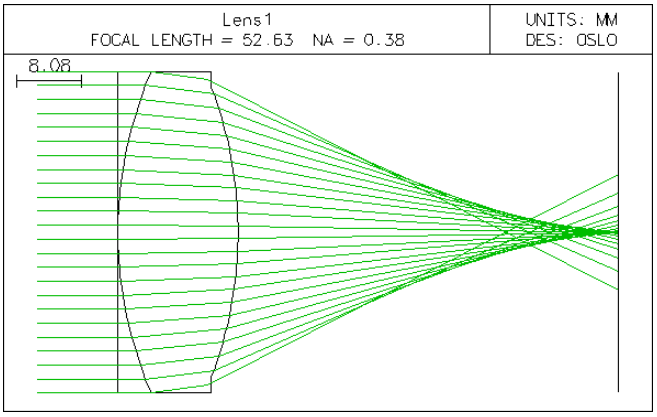

Figure 3 demonstrates the effect of spherical aberration by showing the varying points at which rays cross the optical axis after refraction. Graphic taken from [5].

By analysing the spot diagram at the paraxial focal plane, spherical aberration is apparent. In order to estimate the size of the geometrical focus, the RMS displacement of each ray from the optical axis is calculated for the beam of rays at the output plane. The larger the RMS, the blurrier the image appears. This emphasises the importance of producing a lens that reduces the effects of spherical aberration. In theory, a plano-convex lens set up in the inverse orientation should result in a smaller RMS than in the converse position. This occurs as the deviation of the marginal rays is minimised when the curved surface faces the incident light. [6] The results of this report agree with this theory, as discussed in Section IV Part C. The ray diagrams for these scenarios are shown in Figure 4.

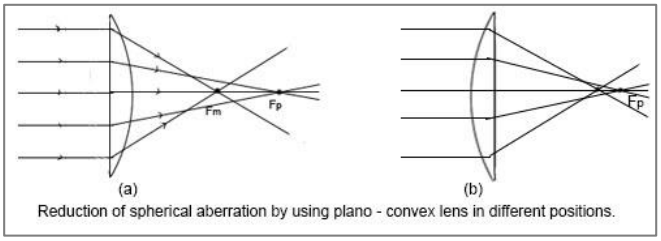

Figure 4 shows the ray diagram for a plano-convex lens in two different positions. Graphic taken from [7].

E. Diffraction scale

The optical ray tracer modelled in this project makes use of geometric optics, which ignores the effects of diffraction. This model works best for a narrow beam, which is well approximated by the paraxial approximation. It seems logical then to use beams with a very small radius. This is acceptable up to a limit, beyond which the rays will no longer converge as suggested by the ray tracer. This limit can be found by comparing the RMS of the beam, calculated using the paraxial approximation, with the diffraction scale calculated using the equation:

$$diffraction\ scale = \frac{\lambda f}{D} \tag{5}$$

where λ is the wavelength, f is the focal length, and D is the diameter of the input bundle of rays. [2]

If the RMS is greater than the diffraction scale, rays will converge as shown. The diffraction limit is found for each lens, with comparison graphs given in Section IV.

III. Method

The 3D optical ray tracer is simulated using an object-oriented method. By designing the rays and the optical elements as objects within the program, analysis is performed on the objects to consider the propagation of a bundle of rays through spherical elements.

A. Rays

A ray is represented by an array of 3D Cartesian points that tracks the path of the ray through the optical system. The direction vector of each ray is also stored as an accessible dictionary of coordinates. Methods are written to append these location and direction lists and to return them to be mapped on a graph or used in a function.

B. Optical Elements

The parameters, as described in Section II Part A, are used to define the optical elements in the system. Methods are included within the object classes to determine the interception points – calculated using vector algebra – and the effect the object has on the propagation of the ray.

The spherical surfaces of focus in this report include;

- a single concave lens,
- a plano-convex singlet lens,
- the plano-convex singlet lens in the inverse orientation.

C. Snell's Law

A function is written independently to describe Snell's law refraction and the effect this has on the direction of a ray. This is implemented in the class for a spherical surface. Rays then propagate to the output plane, set to be at the focal point for converging rays, and an arbitrary point for diverging rays. A special instance is described for a ray subject to total internal reflection such that the path of the ray is ignored unless it undergoes refraction and reaches the output plane.

D. Focal Point

Initially, for a single spherical surface, the focal point is calculated using the lensmaker's equation, given in Equation 4. However, as more elements are added to the optical system and the ray paths complicate, the focal point calculation is replaced by a paraxial approximation method. This tracks the path of a single paraxial ray and locates the point at which it crosses the optical axis, which becomes the new position of the output plane.

E. Spot Diagrams

By mapping the x- and y-coordinates of the rays at the output plane, the spot diagram at the paraxial focal point is plotted. Further to this, the RMS for the spot radius is calculated such that the effect of the different optical element set-ups can be compared.

F. Diffraction Limit

Using Equation 5 and the parameters set for the optical system, the diffraction scale is calculated for the initial input beam. Additionally, the relationship of the beam radius with the diffraction scale and the RMS of the spot radius is plotted to find the diffraction limit, as shown in the graphs in Section IV Part D.

IV. Results & Discussion

The light rays have a wavelength, λ, of 588 nm. The input beam diameter is 10 mm. The bundle layout is set up so that the rays are uniformly spread, as shown in Figure 5.

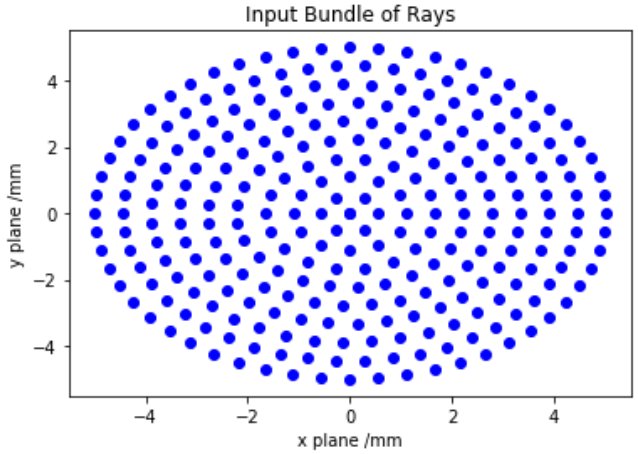

Figure 5 shows each ray in the input beam, arranged at uniform distance to each other and with an outer ring radius of 5 mm. This is the ray bundle which is propagated through the different optical elements.

A. Single Spherical Refracting Surface

The dimensions for this surface are given in Table 1, along with the calculated results for the RMS of the spot radius and the diffraction scale for the input beam.

Single Spherical Refracting Surface	
Curvature /mm:	- 0.03
n_1*:*	1.0
n_2*:*	1.5
RMS (paraxial approx.) /mm:	14.7×10^{-3}
Diffraction Scale /mm:	5.88×10^{-3}

Table 1 gives the dimensions of the single spherical refracting surface, including its curvature, the refractive indices on either side of it, the RMS of the spot radius at the paraxial focus, and the diffraction scale.

As discussed in Section II Part A, the negative curvature shows that this lens is concave. Hence as the lens has a greater refractive index than the air, the rays

are expected to converge to a single point. The path of the rays, shown in Figure 6, indeed shows this to be true.

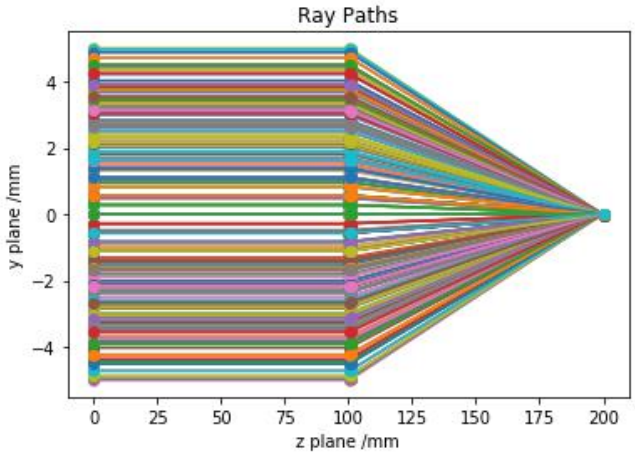

Figure 6 shows how the rays propagate through the optical system containing a single concave lens.

The lens is positioned at 100 mm, with its centre along the optical axis. The paraxial focal point is calculated to be at 200 mm. As the radius of the beam is not larger than the aperture radius, all rays propagate through the lens to the output plane.

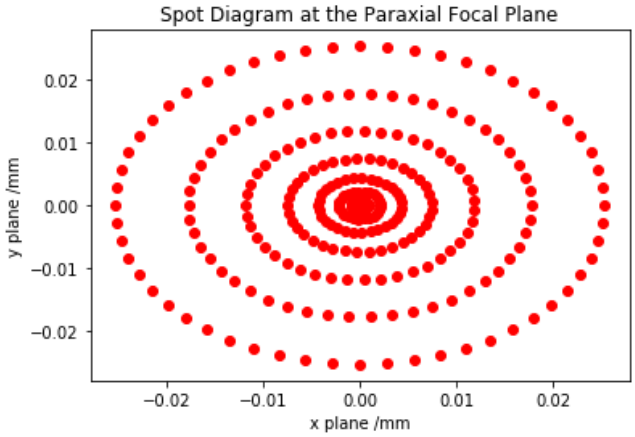

Figure 7 gives the spot diagram at the output plane, located at the paraxial focal point for rays propagated through the concave lens.

However, the rays do not converge to a single point, as shown by the spot diagram at the output plane in Figure 7. The theory given in Section II Part D verifies these results, which demonstrate the effects of spherical aberration. As given in Table 1, the RMS of the distance of each ray from the optical axis is 14.7×10^{-3} mm. This gives the size of the geometrical focus.

B. Plano-Convex Singlet Lens with the Plane Surface Facing the Input

The dimensions for this lens are given in Table 2.

Plano-Convex Singlet Lens	
Curvature /mm:	0.02
$n_1 = n_{air}$:	1.0
$n_2 = n_{glass}$:	1.5168

Table 2 gives the dimensions of the plano-convex singlet lens, including its curvature and the refractive indices on either side of it.

The distance between the convex surface and the planar surface is 5 mm. This set-up is equivalent to a light beam travelling through a glass plano-convex lens with a maximum width of 5 mm.

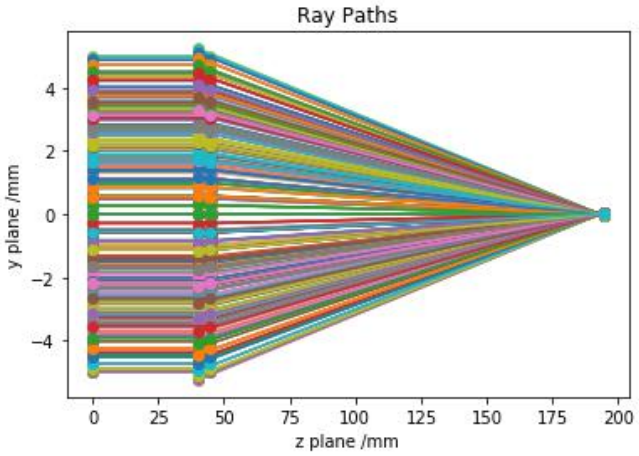

Figure 8 shows how the rays propagate through the optical system containing a plano-convex singlet lens with the plane surface facing the input.

In Figure 8, the two surfaces can be seen from the row of points at 40 and 45 mm. As with the single concave lens, the rays converge but not ideally. The paraxial focal point is calculated to be at 194 mm. This is much further from the lens than in the case of the single concave lens. The spot diagram at the output plane is given in Figure 9.

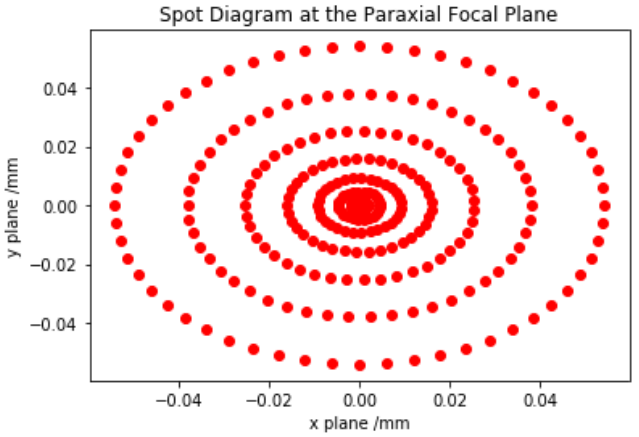

Figure 9 gives the spot diagram at the output plane, located at the paraxial focal point for rays propagated through the plano-convex singlet lens with the plane surface facing the input.

The effects of spherical aberration are strikingly similar to that shown for the single concave lens, with

the main difference being the size of the geometrical focus. The plano-convex lens gives a much larger RMS result, suggesting it produces greater aberrations than the single concave lens. This is considered further in Part C.

C. Plano-Convex Singlet Lens with the Convex Surface Facing the Input

Here, the orientation of the plano-convex lens is flipped such that the convex surface faces the incident rays. The dimensions stay the same as those given in Table 2 and the path of the rays is mapped in Figure 10.

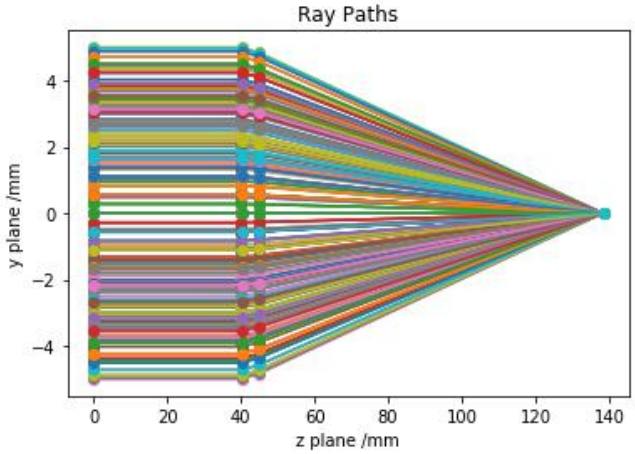

Figure 10 shows how the rays propagate through the optical system containing a plano-convex singlet lens with the convex surface facing the input.

Compared to the previous set-up, the inverse orientation clearly makes a large difference to the positioning of the paraxial focal point, which now lies at 138 mm. The focal distance shown here is much smaller than that given for the alternate orientation, but it is very similar to the focal length of the single concave lens. The effect on the spot diagram is show in Figure 11.

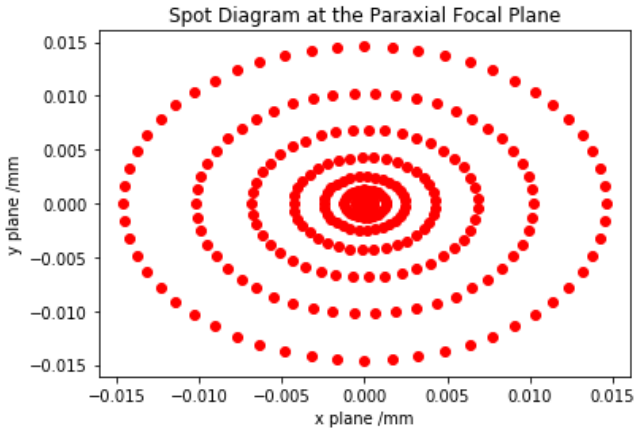

Figure 11 gives the spot diagram at the output plane, located at the paraxial focal point for rays propagated through the plano-convex singlet lens with the convex surface facing the input.

Again, the spot diagram is very similar in layout, except for the size. The size of the geometric focus is compared for both orientations of the plano-convex surface in Table 3.

Plano-Convex Singlet Lens:	**Plane Surface Facing the Input**	**Convex Surface Facing the Input**
RMS (paraxial approx.) /mm:	31.5×10^{-3}	8.50×10^{-3}
Diffraction Scale /mm:	8.78×10^{-3}	5.79×10^{-3}

Table 3 compares the RMS of the distance of each ray from the optical axis at the paraxial focal point, and the diffraction scale, for each orientation of the plano-convex singlet lens.

It is clear from these results that the inverse orientation produces a much smaller RMS spot radius. Physically, this means that the inverse plano-convex lens would produce a clearer image than when set up in the other orientation. However, the diffraction scale is much closer in magnitude to the size of the geometric focus. Additionally, as expected from the similarity in focal length, the diffraction scale for the inverse plano-convex lens is very similar to that of the single concave lens. The effect of the diffraction scale on the reliability of the optical models is discussed in Part D.

D. The Diffraction Limit

Beyond the diffraction limit, the beam no longer converges and instead diffracts and diverges. In this computational model the effect is not shown as the functions are based off geometrical properties. The diffraction limit provides the point at which this geometric model breaks down and the simulation can no longer be used to represent the light propagation. The diffraction limit is found and compared for each optical scenario, with the graphs given in Figure 12.

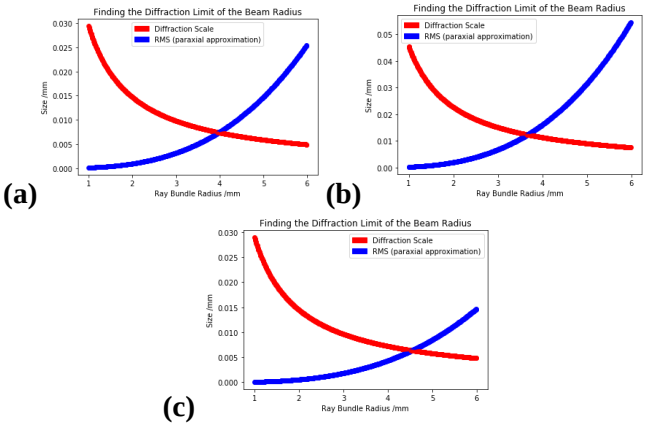

Figure 12 shows the relationship of the beam radius with the diffraction scale and the RMS of the spot radius for the (a) single concave surface, (b) plano-convex lens, and (c) inverse plano-convex lens.

By finding the point at which the beam radius is equivalent in magnitude to the diffraction scale, the diffraction limit is identified. The values for each lens set-up are given in Table 4.

Lens:	**Diffraction Limit of Beam Radius /mm**
Single Concave Surface	3.98
Plano-Convex	3.67
Inverse Plano-Convex	4.54

Table 4 compares the diffraction limit for each lens set-up.

The results here show that whilst the inverse plano-convex lens produces the best image, it is also the most restricted by the diffraction limit.

V. CONCLUSION

This report details the simulation of an optical ray tracer and shows that its results strongly agree with the theory for an optical system. Different systems are compared by considering the clarity of the image they produce, determined by the extent at which they converge to a single point at the paraxial focal point. Discussion of the diffraction scale is given to consider the limit of the geometrical assumptions used in this program.

The code used to build this model could be improved by considering different focal points and moving past the paraxial approximation. Additionally, the consideration of the diffraction limit could be furthered by considering the effect of varying lens curvature, rather than beam diameter. This could then be implemented to produce a best-form lens with the ideal curvature to produce the smallest spot size possible before diffraction effects take over.

VI. REFERENCES

[1] Freniere, E. R., Tourtellott, J., "Brief history of generalized ray tracing", Proc. SPIE 3130, Lens Design, Illumination, and Optomechanical Modeling, (25 September 1997); doi: 10.1117/12.284059; https://doi.org/10.1117/12.284059

[2] Paterson, C., Kingham, R., “Imperial College Physics Y2 Computing - Short Projects (v2.1.1)”. Imperial College London. (Last updated: 2018)

[3] Scratchapixel 2.0, “ Reflection, Refraction and Fresnel”, accessed online 03/04/19, available: https://www.scratchapixel.com/lessons/3d-basic-rendering/introduction-to-shading/reflection-refraction-fresnel

[4] Hecht, E., “Optics (2nd ed.)”, Addison Wesley, (1987); ISBN 978-0-201-11609-0.

[5] Electron6, “Aberration”, accessed online 03/04/19, available: http://electron6.phys.utk.edu/optics421/modules/m2/aberration.htm

[6] The Global Tutors, “Reducing Spherical Aberration”, accessed online 03/04/19, available: https://www.theglobaltutors.com/Homework-Help/optics-homework-help/reducing-spherical-aberration

[7] KulLabs, “Spherical Aberration in a Lens and Scattering of Light”, accessed online 03/04/19, available: https://www.kullabs.com/classes/subjects/units/lessons/notes/note-detail/1764

Note: All figures were created or taken by Isabelle Grenville unless otherwise stated.